

**Supporting Information**

**Efficient Alkaline Hydrogen Evolution on Atomically Dispersed Ni-N<sub>x</sub> Species  
Anchored Porous Carbon with Embedded Ni Nanoparticles by Accelerating Water  
Dissociation Kinetics**

Chaojun Lei,<sup>a</sup> Yu Wang,<sup>d</sup> Yang Hou,<sup>\*a</sup> Pan Liu,<sup>e</sup> Jian Yang,<sup>a</sup> Tao Zhang,<sup>b</sup> Xiaodong Zhuang,<sup>b</sup>  
Mingwei Chen,<sup>e</sup> Bin Yang,<sup>a</sup> Lecheng Lei,<sup>a</sup> Chris Yuan,<sup>f</sup> Ming Qiu,<sup>\*c</sup> Xinliang Feng<sup>\*b</sup>

<sup>a</sup> Key Laboratory of Biomass Chemical Engineering of Ministry of Education, College of  
Chemical and Biological Engineering, Zhejiang University, Hangzhou 310027, China. E-  
mail: [yhou@zju.edu.cn](mailto:yhou@zju.edu.cn)

<sup>b</sup> Center for Advancing Electronics Dresden (cfaed) & Department of Chemistry and Food  
Chemistry, Technische Universitaet Dresden, 01062 Dresden, Germany.  
E-mail: [xinliang.feng@tu-dresden.de](mailto:xinliang.feng@tu-dresden.de)

<sup>c</sup> Institute of Nanoscience and Nanotechnology, College of Physical Science and Technology,  
Central China Normal University, Wuhan 430079, China.  
E-mail: [qium@mail.ccnu.edu.cn](mailto:qium@mail.ccnu.edu.cn)

<sup>d</sup> Shanghai Synchrotron Radiation Facility, Shanghai Institute of Applied Physics, Chinese  
Academy of Sciences, Shanghai 201204, China

<sup>e</sup> WPI Advanced Institute for Materials Research, Tohoku University, Sendai 980-8577, Japan  
& CREST, JST, 4-1-8 Honcho Kawaguchi, Saitama 332-0012, Japan

<sup>f</sup> Department of Mechanical and Aerospace Engineering, Case Western Reserve University,  
10900 Euclid Ave, Cleveland, OH 44106, United States

## 26 **Experimental Section**

### 27 **Synthesis of Ni NP|Ni-N-C**

28 For the synthesis of Ni NP|Ni-N-C, 0.07 g  $\text{NiCl}_2 \cdot 6\text{H}_2\text{O}$  and 0.35 g dicyanamide were  
29 dissolved in 20 mL water under stirring and then transferred into a Teflon-lined stainless steel  
30 autoclave. The autoclave was heated to 200 °C and maintained for 4 h. The resulting powder  
31 was pyrolyzed at 900 °C for 3 h under Ar atmosphere. The pyrolyzed sample was further  
32 soaked in 0.5 M  $\text{H}_2\text{SO}_4$  for 10 h to remove accessible Ni species.

### 33 **Synthesis of Ni NP|Ni-N-C after substantial acid etching (Ni-N-C)**

34 For the synthesis of Ni-N-C, 0.07 g  $\text{NiCl}_2 \cdot 6\text{H}_2\text{O}$  and 0.35 g dicyanamide were dissolved in 20  
35 mL water under stirring and then transferred into a Teflon-lined stainless steel autoclave. The  
36 autoclave was heated to 200 °C and maintained for 4 h. The resulting powder was pyrolyzed  
37 at 900 °C for 3 h under Ar atmosphere. The pyrolyzed sample was further soaked in 0.5 M  
38  $\text{H}_2\text{SO}_4$  for 48 h to remove the Ni-containing nanoparticles.

### 39 **Synthesis of Ni NP**

40 For the synthesis of Ni NP, 0.07 g  $\text{NiCl}_2 \cdot 6\text{H}_2\text{O}$  and 0.35 g dicyanamide were dissolved in 20  
41 mL water under stirring and then transferred into a Teflon-lined stainless steel autoclave. The  
42 autoclave was heated to 200 °C and maintained for 4 h. The resulting powder was pyrolyzed  
43 at 900 °C for 3 h under Ar atmosphere. The pyrolyzed sample was further soaked in 0.5 M  
44  $\text{H}_2\text{SO}_4$  for 10 h to remove accessible Ni species. The obtained Ni NP|Ni-N-C powder was  
45 heated to 600 °C and maintained for 2 h under air atmosphere. The resulting product was  
46 finally annealed in mixture atmosphere of Ar/ $\text{H}_2$  at 300 °C for 2 h to generate Ni NP.

### 47 **Synthesis of Ni NP|Ni-N-C/EG**

48 The EG was firstly prepared by anodization of graphite foil in 0.1 M  $(\text{NH}_4)_2\text{SO}_4$  solution with  
49 a Pt foil as counter electrode under 10 V for 15 s.<sup>[1]</sup> Next, the obtained EG was immersed into  
50 20 mL mixture solution of 0.07 g  $\text{NiCl}_2 \cdot 6\text{H}_2\text{O}$  and 0.35 g dicyanamide, and further transferred  
51 into a Teflon-lined stainless steel autoclave. The autoclave was heated to 200 °C and

maintained for 4 h. Finally, the resulting electrode was pyrolyzed at 900 °C for 3 h under Ar atmosphere, followed by acid etching treatment with 0.5 M H<sub>2</sub>SO<sub>4</sub> for 10 h to remove accessible Ni species. The loading amount of Ni NP|Ni-N-C/EG on graphite foil was ~ 0.24 mg cm<sup>-2</sup>.

#### **Synthesis of Ni NP|Ni-N-C/EG (700 °C)**

The EG was immersed into 20 mL mixture solution of 0.07 g NiCl<sub>2</sub>•6H<sub>2</sub>O and 0.35 g dicyanamide, and further transferred into a Teflon-lined stainless steel autoclave. The autoclave was heated to 200 °C and maintained for 4 h. Finally, the resulting electrode was pyrolyzed at 700 °C for 3 h under Ar atmosphere, followed by acid etching treatment with 0.5 M H<sub>2</sub>SO<sub>4</sub> for 10 h to remove accessible Ni species.

#### **Synthesis of Ni NP|Ni-N-C/EG (800 °C)**

The EG was immersed into 20 mL mixture solution of 0.07 g NiCl<sub>2</sub>•6H<sub>2</sub>O and 0.35 g dicyanamide, and further transferred into a Teflon-lined stainless steel autoclave. The autoclave was heated to 200 °C and maintained for 4 h. Finally, the resulting electrode was pyrolyzed at 800 °C for 3 h under Ar atmosphere, followed by acid etching treatment with 0.5 M H<sub>2</sub>SO<sub>4</sub> for 10 h to remove accessible Ni species.

#### **Synthesis of Ni NP|Ni-N-C/EG (1000 °C)**

The EG was immersed into 20 mL mixture solution of 0.07 g NiCl<sub>2</sub>•6H<sub>2</sub>O and 0.35 g dicyanamide, and further transferred into a Teflon-lined stainless steel autoclave. The autoclave was heated to 200 °C and maintained for 4 h. Finally, the resulting electrode was pyrolyzed at 1000 °C for 3 h under Ar atmosphere, followed by acid etching treatment with 0.5 M H<sub>2</sub>SO<sub>4</sub> for 10 h to remove accessible Ni species.

#### **Synthesis of Ni-N-C/EG**

The EG was immersed into 20 mL mixture solution of 0.07 g NiCl<sub>2</sub>•6H<sub>2</sub>O and 0.35 g dicyanamide, and further transferred into a Teflon-lined stainless steel autoclave. The autoclave was heated to 200 °C and maintained for 4 h. Finally, the resulting electrode was

pyrolyzed at 900 °C for 3 h under Ar atmosphere, followed by acid etching treatment with 0.5 M H<sub>2</sub>SO<sub>4</sub> for 48 h to remove the Ni-containing nanoparticles. The loading amount of Ni-N-C/EG on graphite foil was ~ 0.16 mg cm<sup>-2</sup>.

#### **Synthesis of Ni NP/EG**

The EG was immersed into 20 mL mixture solution of 0.07 g NiCl<sub>2</sub>•6H<sub>2</sub>O and 0.35 g dicyanamide, and further transferred into a Teflon-lined stainless steel autoclave. The autoclave was heated to 200 °C and maintained for 4 h. The resulting electrode was then pyrolyzed at 900 °C for 3 h under Ar atmosphere, followed by acid etching treatment with 0.5 M H<sub>2</sub>SO<sub>4</sub> for 10 h to remove accessible Ni species. The obtained Ni NP|Ni-N-C/EG electrode was heated to 600 °C and maintained 600 °C for 2 h under air atmosphere. The resulting electrode was finally annealed in mixture atmosphere of Ar/H<sub>2</sub> at 300 °C for 2 h to generate Ni NP/EG. The loading amount of Ni NP/EG on graphite foil was ~ 0.10 mg cm<sup>-2</sup>.

#### **Synthesis of physical mixture of Ni NP and Ni-N-C supported on EG**

As a reference, the Ni NP and Ni-N-C powders were ground together to form the physical mixture of Ni NP and Ni-N-C. The obtained mixture was further loaded on the surface of EG with the loading amount of ~ 0.24 mg cm<sup>-2</sup> (physical mixture/EG).

#### **Characterization**

The morphology was characterized by field emission scanning electron microscope (FESEM, Carl Zeiss NVision 40), transmission electron microscopy (TEM, JEOL JEM-2001F and Carl Zeiss, Libra 120), high-resolution TEM (HRTEM, JEOL JEM-2001F and Carl Zeiss, Libra 120), high angle annular dark-field scanning TEM (HAADF-STEM), and energy dispersive spectra (EDX, JEOL JEM-2001F and Carl Zeiss, Libra 120). X-ray diffraction (XRD) pattern was performed on a Bruker D8 Advance powder diffractometer. Fourier transform infrared spectroscopy (FTIR) was carried out using a BRUKER TENSOR II spectrometer. Raman measurement was carried out on an NTEGRA Spectra system (NT-MDT). Thermogravimetric curve was recorded on a TA SDT 2960 thermoanalyzer. The Ni contents

104 of samples before and after HER reactions were recorded with inductively coupled plasma  
105 mass spectrometry (ICP-MS). Nitrogen sorption isotherms were measured with a Quadrasorb  
106 Adsorption Instrument. X-ray photoelectron spectra (XPS) were performed on an AXIS Ultra  
107 DLD system (Kratos). The contact wetting angles were characterized on a "DSA-10" Kruss  
108 goniometer. X-ray absorption near edge structure (XANES) and X-ray absorption fine  
109 structure (EXAFS) measurements were tested on the BL10C beam line of Pohang light source  
110 (PLS- II, Korea).

### 111 **Electrochemical measurements**

112 Electrochemical measurements of as-prepared samples were performed using CHI 760 E  
113 electrochemical analyzer in a three-electrode configuration, which was operated with a  
114 graphite rod and an Ag/AgCl electrode as counter electrode and reference electrode,  
115 respectively. Polarization curves were obtained with a scan rate of  $1 \text{ mV s}^{-1}$  in 1.0 M KOH  
116 electrolyte. Long-term durability test was performed using chronoamperometric measurement.  
117 All of the potentials are referenced to the reversible hydrogen electrode (RHE), and voltages  
118 are  $iR$  corrected unless noted. The solution resistances are measured by electrochemical  
119 impedance spectroscopy (EIS) in this work.<sup>[2]</sup>

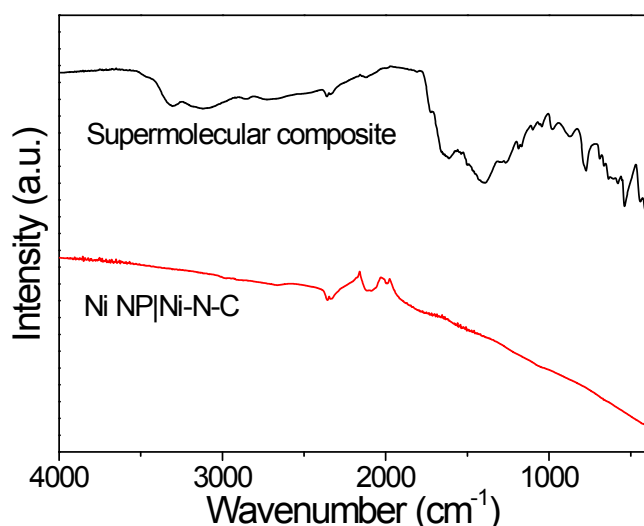
120 For overall-water-splitting tests, the electrodes were directly used as both cathode and anode  
121 with a mass loading amount of  $0.24 \text{ mg cm}^{-2}$ . Polarization curves were obtained with a scan  
122 rate of  $1 \text{ mV s}^{-1}$  in 1.0 M KOH electrolyte. Durability of the samples was assessed via using  
123 constant current electrolysis. For comparison, the commercial Ir/C and Pt/C catalysts that  
124 were drop-dried onto the EG foil with mass loading amount of  $0.24 \text{ mg cm}^{-2}$ , respectively  
125 were measured under the same experimental conditions.

### 126 **First-principles calculations**

127 All first-principles-based calculations were conducted by applying the Cambridge Serial Total  
128 Energy Package (CASTEP) in Material Studio which performs the density functional theory  
129 (DFT) plane-wave pseudopotential method to carry out first principles quantum mechanics

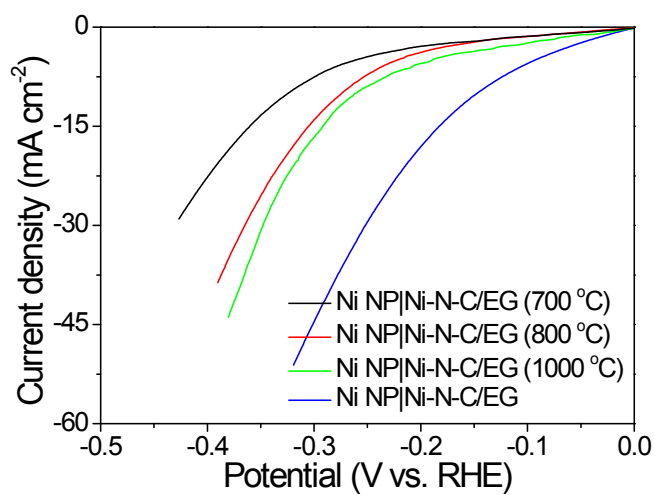
130 calculations. In the calculation, the generalized gradient approximation (GGA) within  
 131 Perdew–Burke–Ernzerhof (PBE) form was used as the exchange–correlation function. The  
 132 convergence tests of the total energy with respect to the k-points sampling and the energy-  
 133 cutoff were carefully examined, using  $3 \times 3 \times 1$  Monkhorst-Pack k-points grid and a 800 eV  
 134 energy-cutoff for plane-wave expansion. Valence states used were Ni-3s<sup>2</sup>3p<sup>6</sup>3d<sup>8</sup>4s<sup>2</sup>, C-2s<sup>2</sup>2p<sup>2</sup>,  
 135 N-2s<sup>2</sup>2p<sup>3</sup>, O-2s<sup>2</sup>2p<sup>4</sup> and H-1s<sup>1</sup>. In the super-cell configuration, a sufficiently large vacuum slab  
 136 (about 15 Å) was maintained. The SCF tolerance was setup to  $1 \times 10^{-6}$  eV·atom<sup>-1</sup> for the  
 137 geometrical optimization and phonon calculations.

138



139

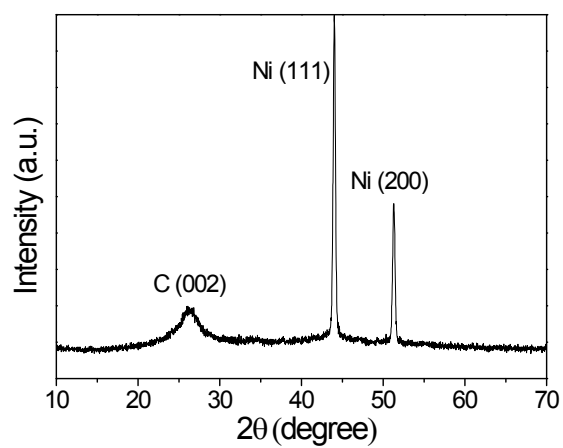
140 **Figure S1.** FTIR spectra of Ni NP|Ni-N-C and hydrothermally prepared supermolecular  
 141 composite of dicyandiamide and Ni salt.



143

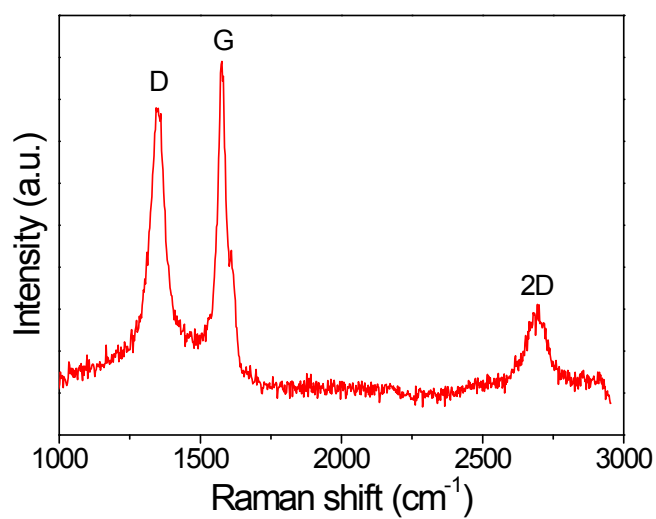
144 **Figure S2.** Polarization curves of Ni NP|Ni-N-C/EG, Ni NP|Ni-N-C/EG (700 °C), Ni NP|Ni-  
145 N-C/EG (800 °C), and Ni NP|Ni-N-C/EG (1000 °C) in 1.0 M KOH.

146



147

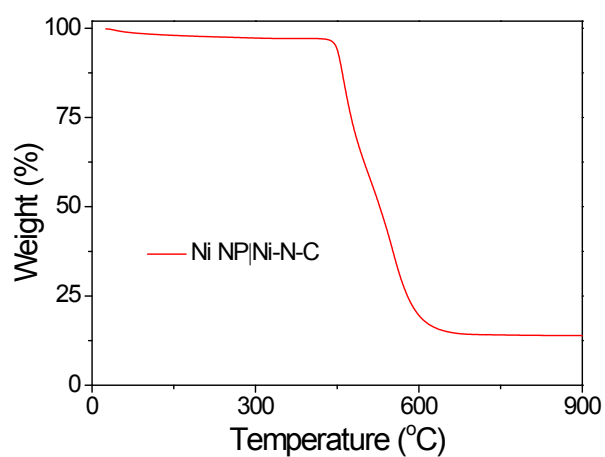
148 **Figure S3.** XRD pattern of Ni NP|Ni-N-C.



150

151 **Figure S4.** Raman spectrum of Ni NP|Ni-N-C.

152



153

154 **Figure S5.** TGA curve of Ni NP|Ni-N-C under flowing air.

155

156 The TGA result also reveals that the content of Ni species in the Ni NP|Ni-N-C is about 11.8  
 157 wt.%, considering that the final product can be nickel oxide.



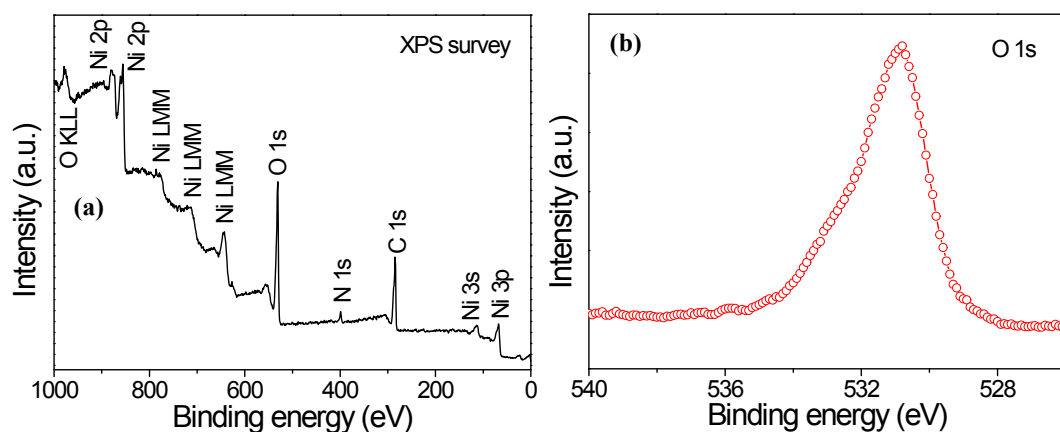


**Figure S6.** The XPS survey spectrum (a) and high-resolution O 1s XPS spectrum (b) of Ni NP|Ni-N-C.

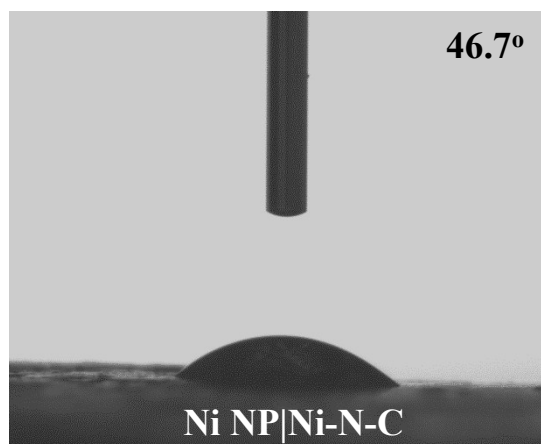


**Figure S7.** Contact wetting angel of Ni NP|Ni-N-C.

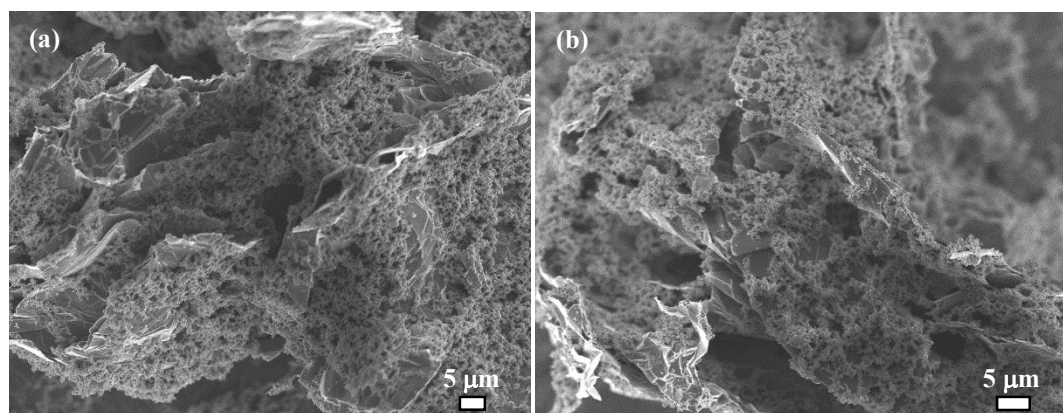
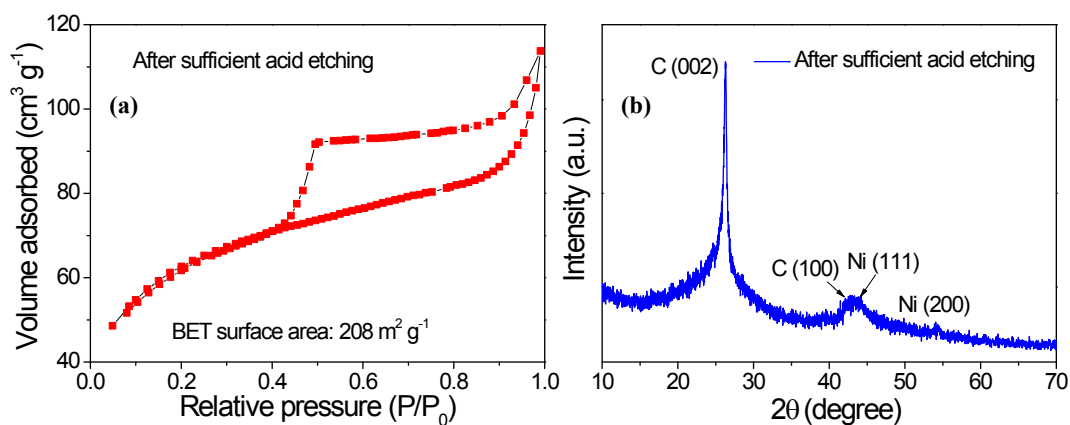


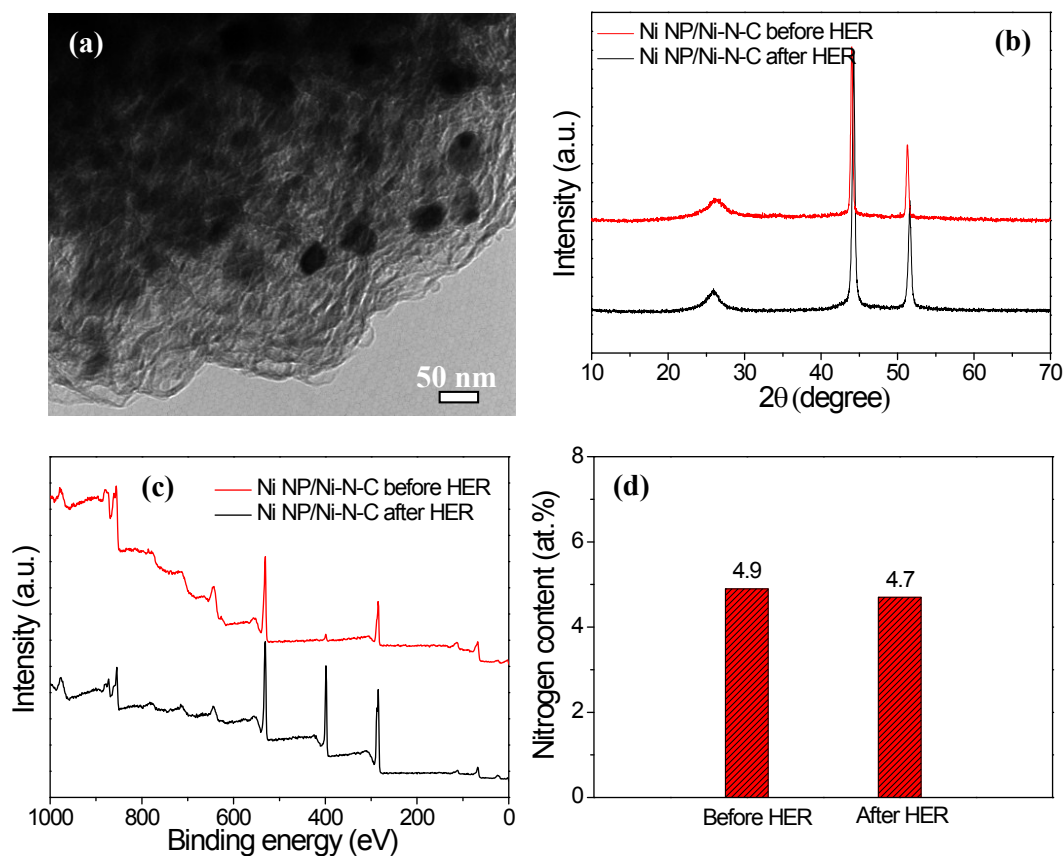
**Figure S8.** (a-b) FESEM images of Ni NP|Ni-N-C/EG.



168

169 **Figure S9.** (a) N<sub>2</sub> adsorption-desorption isotherm and (b) XRD pattern of Ni NP|Ni-N-C after  
170 sufficient acid etching treatment (Ni-N-C).

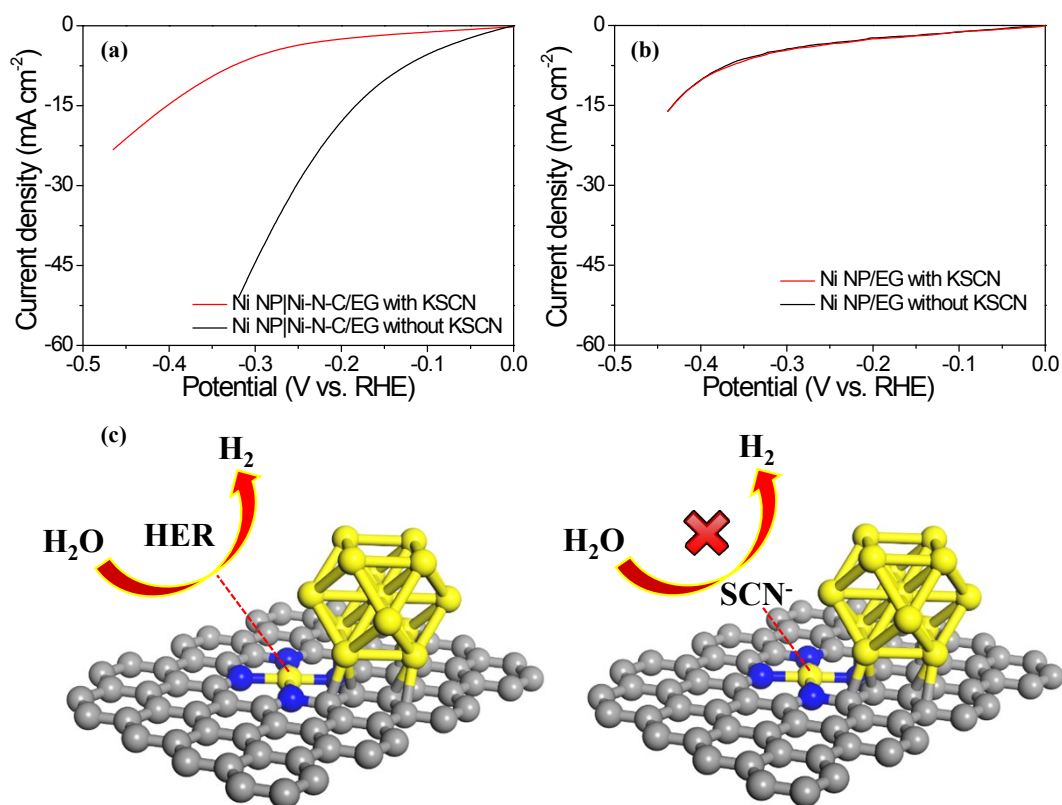
171



172

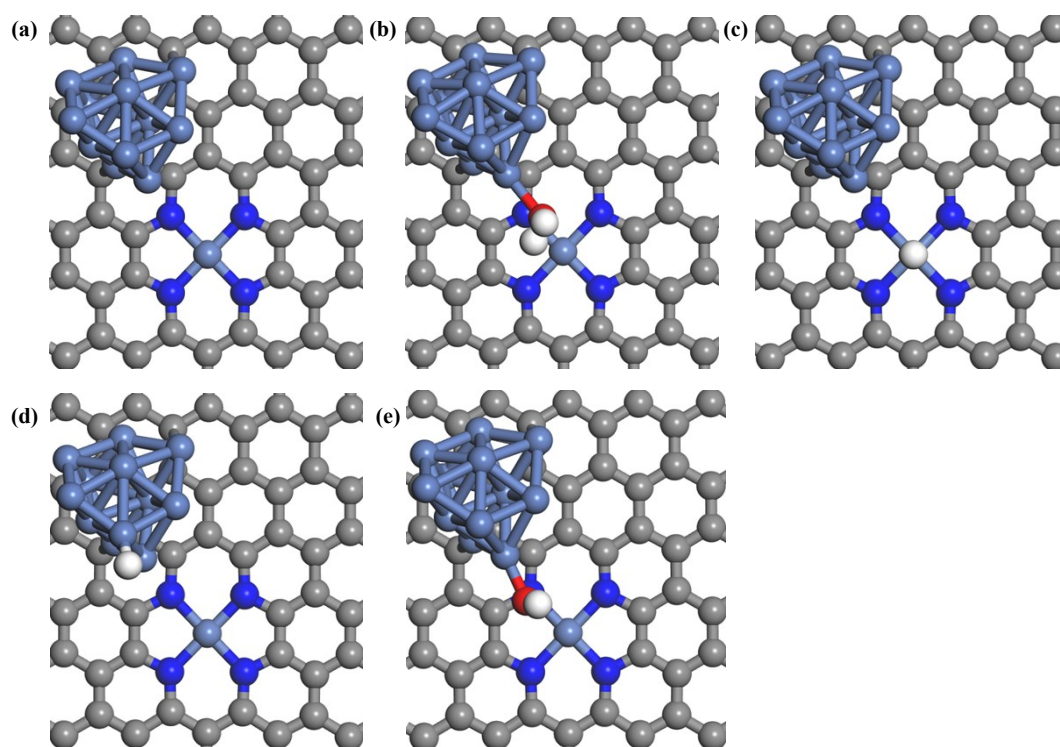
173 **Figure S10.** (a) TEM image of Ni NP|Ni-N-C after HER test, (b) XRD patterns of Ni NP|Ni-  
174 N-C before and after HER tests, (c) XPS survey spectra of Ni NP|Ni-N-C before and after  
175 HER tests, and (d) N-content column bar graph of Ni NP|Ni-N-C before and after HER tests.

176



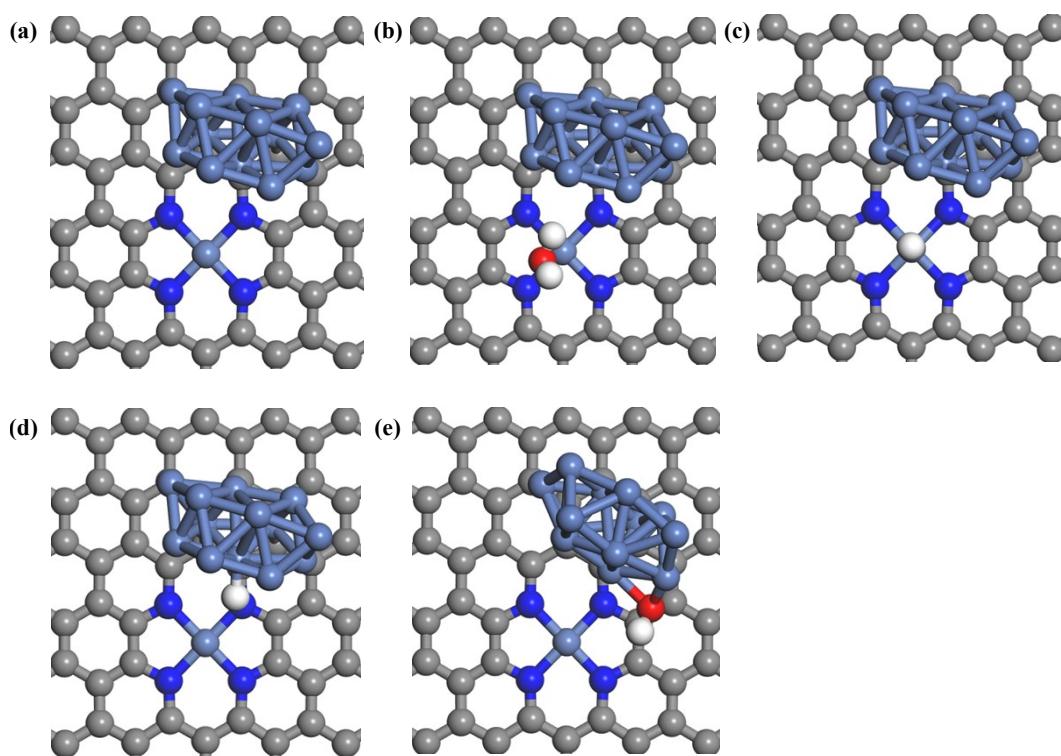
177

178 **Figure S11.** HER polarization curves of Ni NP|Ni-N-C/EG (a) and Ni NP/EG (b) with and  
 179 without 10 mM KSCN in 1.0 M KOH. (c) Illustrations of Ni centers blocked by the  $\text{SCN}^-$   
 180 ions.



182

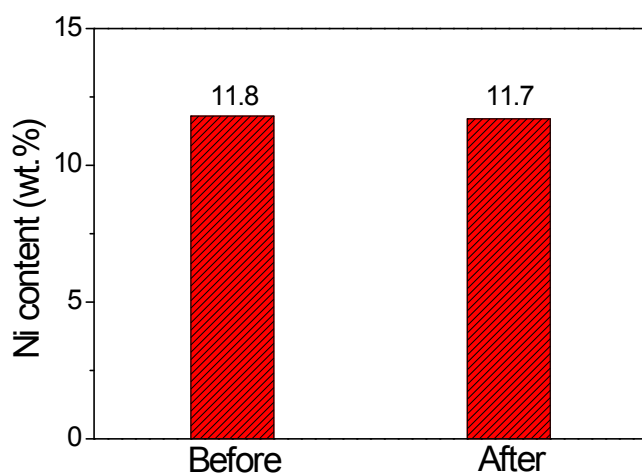
183 **Figure S12.** DFT calculated models (Volmer-Tafel-Heyrovsky mechanism) for NiN<sub>4</sub>/NP1.



185

186 **Figure S13.** DFT calculated models (Volmer-Tafel-Heyrovsky mechanism) for NiN<sub>4</sub>|NP3.

187



188

189 **Figure S14.** Ni content of Ni NP|Ni-N-C before and after HER stability test, as quantified by  
190 ICP-MS spectrometry.

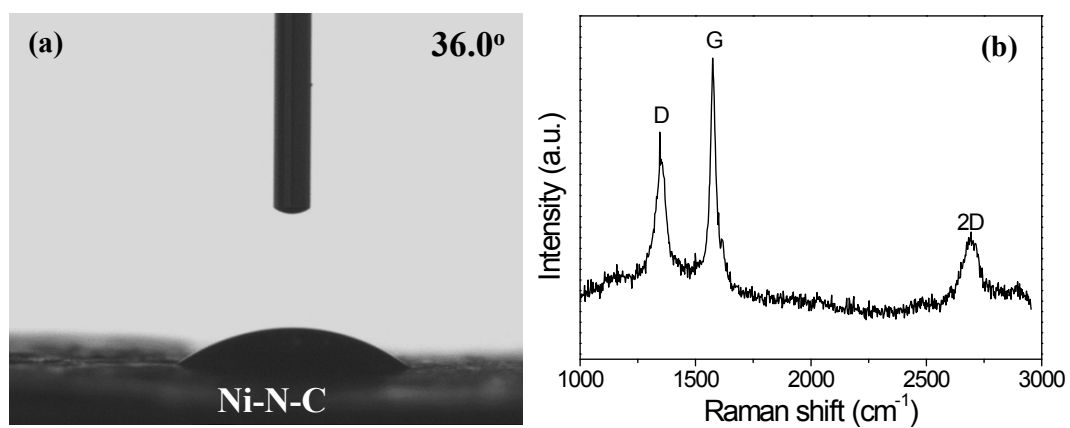


**Figure S15.** (a) Contact wetting angel and (b) Raman spectrum of Ni NP|Ni-N-C after sufficient acid etching treatment (Ni-N-C).

196 **Table S1.** Comparison of HER performance of Ni NP|Ni-N-C with some representative  
 197 heteroatom-doped nanocarbon materials and transition-metal-based compounds.

Author	Catalyst (Loading density, mg cm <sup>-2</sup> )	Current density (J)	Potential at the correspondin g J	Electrolyte
<b>This work</b>	<b>Ni NP Ni-N-C (0.24 mg cm<sup>-2</sup>)</b>	<b>10 mA cm<sup>-2</sup></b>	<b>147 mV</b>	<b>1.0 M KOH</b>
Adv. Mater. 2015, 27, 3175	PCPTF (0.1 mg cm <sup>-2</sup> )	10 mA cm <sup>-2</sup>	~370 mV	1.0 M KOH
Energy Environ. Sci. 2016, 9, 1210	ONPPGC/OCC (0.1 mg cm <sup>-2</sup> )	10 mA cm <sup>-2</sup>	~430 mV	1.0 M KOH
J. Am. Chem. Soc. 2015, 137, 15070	Co-C-N (2.0 mg cm <sup>-2</sup> )	10 mA cm <sup>-2</sup>	~200 mV	1.0 M KOH
Angew. Chem. Int. Ed. 2014, 126, 4461	Co-NRCNTs (0.28 mg cm <sup>-2</sup> )	10 mA cm <sup>-2</sup>	~370 mV	1.0 M KOH
J. Am. Chem. Soc. 2015, 137, 2688	CoO <sub>x</sub> @CN (0.42 mg cm <sup>-2</sup> )	10 mA cm <sup>-2</sup>	235 mV	1.0 M KOH
Adv. Mater. 2016, 28, 6442	Pr <sub>0.5</sub> BSCF (0.232 mg cm <sup>-2</sup> )	10 mA cm <sup>-2</sup>	237 mV	1.0 M KOH
Angew. Chem. Int. Ed. 2015, 54, 12361	Ni <sub>5</sub> P <sub>4</sub> film (13.9 mg cm <sup>-2</sup> )	10 mA cm <sup>-2</sup>	150 mV	1.0 M KOH
J. Am. Chem. Soc. 2013, 135, 9267	Ni <sub>2</sub> P (1.0 mg cm <sup>-2</sup> )	10 mA cm <sup>-2</sup>	210 mV	1.0 M KOH
Chem. Sci. 2016, 7, 1690	CoP/rGO-400 (0.28 mg cm <sup>-2</sup> )	10 mA cm <sup>-2</sup>	~160 mV	1.0 M KOH
J. Am. Chem. Soc. 2014, 136, 7587	CoP/CC (0.92 mg cm <sup>-2</sup> )	10 mA cm <sup>-2</sup>	210 mV	1.0 M KOH
J. Am. Chem. Soc. 2014, 136, 15670	CoSe <sub>2</sub> nanosheets (0.142 mg cm <sup>-2</sup> )	10 mA cm <sup>-2</sup>	320 mV	0.1 M KOH
Angew. Chem. Int. Ed. 2012, 51, 12703	MoB (0.9 mg cm <sup>-2</sup> )	10 mA cm <sup>-2</sup>	~220 mV	1.0 M KOH
Angew. Chem. Int. Ed.	MoS <sub>2+x</sub> /Ni foam	10 mA cm <sup>-2</sup>	210 mV	0.1 M KOH

2015, 127, 674	(0.02 mg cm <sup>-2</sup> )			
Energy Environ. Sci. 2016, 9, 2789	Co-MoS <sub>2</sub> (0.89 mg cm <sup>-2</sup> )	10 mA cm <sup>-2</sup>	200 mV	1.0 M KOH
Energy Environ. Sci. 2016, 9, 2789	MoS <sub>2</sub> nanosheets (0.89 mg cm <sup>-2</sup> )	10 mA cm <sup>-2</sup>	310 mV	1.0 M KOH
Chem. Sci. 2016, 7, 3399	MoC-Mo <sub>2</sub> C (0.14 mg cm <sup>-2</sup> )	10 mA cm <sup>-2</sup>	~150 mV	1.0 M KOH
Nat. Mater. 2016, 15, 197	CoS <sub>x</sub> /MoS <sub>2</sub> (0.05 mg cm <sup>-2</sup> )	5 mA cm <sup>-2</sup>	210 mV	0.1 M KOH
Chem. Sci. 2011, 2, 1262	Amorphous MoS <sub>x</sub> (---)	4 mA cm <sup>-2</sup>	540 mV	0.1 M KOH
Adv. Funct. Mater. 2016, 26, 3314	Ni/NiS (11.04 mg cm <sup>-2</sup> )	10 mA cm <sup>-2</sup>	~220 mV	1.0 M KOH
Nano Energy 2016, 24, 103	NF-Ni <sub>3</sub> Se <sub>2</sub> /Ni (8.87 mg cm <sup>-2</sup> )	10 mA cm <sup>-2</sup>	203 mV	1.0 M KOH
Nano Energy 2016, 29, 37	CoP NPs (0.18 mg cm <sup>-2</sup> )	10 mA cm <sup>-2</sup>	170 mV	1.0 M KOH
J. Mater. Chem. A, 2016, 4, 10114	u-CoP/Ti (6.32 mg cm <sup>-2</sup> )	10 mA cm <sup>-2</sup>	60 mV	1.0 M KOH
Int. J. Hydrogen Energy, 2015, 40, 4727	Ni <sub>3</sub> S <sub>2</sub> /Ni foam (1.5 mg cm <sup>-2</sup> )	10 mA cm <sup>-2</sup>	123 mV	1.0 M KOH

198

## 199 References

- 200 [1] K. Parvez, Z. S. Wu, R. Li, X. Liu, R. Graf, X. Feng, K. Müllen, *Journal of the*  
201 *American Chemical Society* **2014**, 136, 6083.
- 202 [2] M. R. Gao, J. X. Liang, Y. R. Zheng, Y.-F. Xu, J. Jiang, Q. Gao, J. Li, S. H. Yu, *Nat*  
203 *Commun* **2015**, 6.